Enhanced prefrontal nicotinic signaling as evidence of active compensation in Alzheimer's disease models

Saige K Power[1], Sridevi Venkatesan[1], Sarah Qu[1], JoAnne McLaurin[2,3], Evelyn K Lambe[1,4,5]

1. Department of Physiology, Temerty Faculty of Medicine, University of Toronto

2. Department of Laboratory Medicine and Pathobiology, Temerty Faculty of Medicine, University of Toronto

3. Biological Sciences, Hurvitz Brain Sciences Research Program, Sunnybrook Research Institute

4. Department of Obstetrics and Gynaecology, Temerty Faculty of Medicine, University of Toronto

5. Department of Psychiatry, Temerty Faculty of Medicine, University of Toronto

Figures: 5

Supplemental Material: Tables S1 and S2

Keywords: Alzheimer's disease, cognitive reserve, prefrontal cortex, acetylcholine, nicotinic receptors, optogenetics, electrophysiology, acetylcholinesterase inhibitor, compensation

Abstract

Background: Cognitive reserve allows for active compensation during neuropathology. Here, we examine electrophysiological evidence for active compensation in Alzheimer's disease (AD) focusing on the cholinergic signalling pathways in the prefrontal cortex. These pathways are vulnerable to neuropathology in AD and its preclinical models and are essential for attention and executive function.

Methods: We functionally interrogate aspects of the cholinergic system *ex vivo*, in brain slices of prefrontal cortex from two preclinical models: a compound transgenic AD mouse that permits optogenetically-triggered release of endogenous acetylcholine and a transgenic AD rat that closely recapitulates the human trajectory of AD. We then tested the impact of therapeutic interventions to further amplify the compensated responses and preserve the typical kinetic profile of cholinergic signaling.

Results: In two AD models, we find a potentially-compensatory upregulation of functional cholinergic responses above non-transgenic controls after onset of pathology. To identify the locus of this enhanced cholinergic signal, we dissect key pre- and post-synaptic components with pharmacological strategies. We identify a significant and selective increase in post-synaptic nicotinic receptor signalling on prefrontal cortical neurons. To probe the additional impact of therapeutic intervention on the adapted circuit, we test cholinergic and nicotinic-selective pro-cognitive treatments. The inhibition of acetylcholinesterase further enhances endogenous cholinergic responses but greatly distorts their kinetics. Positive allosteric modulation of nicotinic receptors, by contrast, enhances endogenous cholinergic responses and retains their rapid kinetics.

Conclusions: We demonstrate that functional nicotinic compensation occurs within the prefrontal cortex in two AD models. Promisingly, this compensated nicotinic signal can be boosted while preserving its rapid kinetic signature. Taken together, we conclude that cognitive reserve mechanisms act selectively within the prefrontal cholinergic pathway and reveal a new approach for cognitive treatment in AD neuropathology.

Introduction

Cognitive reserve denotes an individual's ability to withstand a higher degree of neurological decline before exhibiting cognitive impairment [1]. Lifestyle factors have been shown to promote cognitive reserve, decreasing risk of dementia and slowing cognitive decline in Alzheimer's disease (AD) [2–4]. The impact of these factors is not limited to disease onset but persists even as neuropathology worsens [5–9]. In fact, cognitive reserve is hypothesized to allow for compensation during neuropathology [10,11], generating a new or stronger response to sustain network recruitment [12,13]. In AD and its preclinical models, there are now several diverse examples of neuronal compensation leading to cognitive maintenance [14,15], but compensatory capacity in the cholinergic system has not been systematically evaluated.

Cholinergic pathways in prefrontal cortex are well positioned to contribute to mechanisms of cognitive reserve in AD. This modulation is essential for attention and executive function [16]. Pro-cholinergic treatments improve cognition preclinically [17–19] and slow cognitive decline clinically [20–23]. While the remodelling of the cholinergic system in AD has been extensively probed, key clinical [24–26] and preclinical studies [27–29] focus on cholinergic neurodegeneration and synapse loss. There has been relatively little functional investigation in early to mid-disease synaptic changes, except in the most swiftly-progressing genetic models of AD that preclude the use of littermate controls [30–39]. To detect and systematically investigate mechanisms of compensatory plasticity, it is essential to use a well-charted model with appropriately-matched non-transgenic controls.

To examine cholinergic signalling in AD, we use optogenetics and whole cell electrophysiology *ex vivo* to investigate prefrontal acetylcholine pathways. In models of AD from two different species, we find a strong and significant upregulation of prefrontal cholinergic responses above non-transgenic levels after onset of pathology. To probe the mechanisms underlying this functional compensation, we systematically manipulated pre- and postsynaptic elements of the cholinergic synapse. We discovered the upregulation is specific to nicotinic receptor signalling. Lastly, we assessed the functional impact of therapeutic interventions, contrasting current standard AD treatment with a novel nicotinic treatment. Both manipulations improve endogenous cholinergic responses, but only the targeted nicotinic treatment preserves the typical rapid timing thought essential for cue detection. Overall, we demonstrate evidence for an active cholinergic mechanism of cognitive compensation that remain accessible to further potentiation with treatment.

Materials & methods

Animals

The University of Toronto Temerty Faculty of Medicine Animal Care Committee approved experiments in accordance with the guidelines of the Canadian Council on Animal Care (protocols #20011123, #20011621, #20011796). TgCRND8 transgenic mice expressing double human amyloid precursor protein Swedish and Indiana mutations (KM670/671NL/V717F) under the Prp gene promoter [40] on a C57BL/6 background were crossed with transgenic mice expressing channelrhodopsin in cholinergic afferents (ChATChR2; RRID:IMSR_JAX:014546, Jackson Laboratory [41]). TgCRND8/ChATChR2 mice were compared to ChATChR2 littermates as controls. Male and female mice were weaned at postnatal day (P)21, separated by sex, and group

housed (2-4 mice per cage) in plastic cages with corn cob bedding, houses for environmental enrichment, with *ad libitum* access to food and water on a 12hr light/dark cycle with lights on at 7:00AM. Mice were used at two age groups based on previously described progression [42–46]: an early to mid-disease group and controls, 3-6 months old (n = 30, mean 4.7 ± 0.2 months), and a later disease group and controls, 7 to 12 months (n = 26, mean 9.9 ± 0.3 months). Groups were balanced for sex and genotype.

TgF344 AD rats expressing the human amyloid precursor protein Swedish mutation (KM670/671NL) and presenilin 1 with exon 9 excised, under the mouse prion promoter [47] were outbred on a Fischer strain. TgF344 AD rats were compared to F344 littermates as controls. Rats were bred at Sunnybrook Research Institute (protocol #22655), and housed in plastic cages with corn cobb bedding, 2 animals per cage, with houses and toys for environmental enrichment, on a 12hr light/dark cycle with *ad libitum* access to food and water. Rats were transferred to the University of Toronto Division of Comparative Medicine and housed for a minimum of 6 weeks before experiments. Rats were used at three age groups based on stages described previously [48–51]:, an age group at 8 months for consideration of early AD and controls (n = 21, mean 8.4 ± 0.2 months), at 12 months for mid-AD and controls (n = 23, mean 12.4 ± 0.2 months), and 18 months for later AD and controls (n = 26, mean 17.6 ± 0.2 months). Groups were balanced for sex and genotype.

Electrophysiology and optogenetics

Animals were anaesthetized with an intraperitoneal injection of chloral hydrate (400mg/kg) and decapitated. The brain was rapidly removed in 4˚C sucrose ACSF (254 mM sucrose, 10 mM D-glucose, 26 mM $NaHCO_3$, 2 mM $CaCl_2$, 2 mM $MgSO_4$, 3 mM KCl, and 1.25 mM Na_2PO_4). The 400uM thick cortical slices of the prefrontal cortex (bregma 2.2-1.1) were obtained on a Dosaka linear slicer (SciMedia). Slices were transferred to a prechamber (automate Scientific) where they recovered for at least 2 Hr in oxygenated (95% O_2, 5% CO_2) ACSF (128 mM NaCl, 10 mM D-glucose, 26 mM $NaHCO_3$, 2 mM $CaCl_2$, 2 mM $MgSO_4$, 3 mM KCl, and 1.25 mM Na_2PO_4) at 30˚C before being used for electrophysiology.

For whole-cell patch-clamp electrophysiology, brain slices were transferred to a chamber mounted on the stage of a BX51WI (Olympus) microscope and perfused with 30 ˚C oxygenated ACSF at 3-4mL/min. Layer 6 pyramidal neurons in the prelimbic and anterior cingulate regions of the medial prefrontal cortex were identified by size, morphology, and proximity to white matter, visualized using infrared differential interference contrast microscopy. Recording electrodes were filled with patch solution containing 120 mM K-gluconate, 5 mM $MgCl_2$, 4 mM K-ATP, 0.4 mM Na_2-GTP, 10 Mm Na_2-phosphocreatine, and 10 mM HEPES buffer adjusted to pH 7.33 with KOH. Data were acquired and low-pass filtered at 20kHz with Axopatch 200b amplifier (Molecular Devices) and Digidata 1440 digitizer and pClamp10.3 acquisition software (Molecular Devices). Responses from a homogenous population of layer 6 regular spiking pyramidal neurons [52,53] were examined in voltage clamp at -75 mV and in current clamp.

To excite channelrhodopsin-containing cholinergic afferents optogenetically (opto-ACh), blue light (470 nm) was delivered in 5ms pulses with an LED (2mW; Thorlabs) through a 60x objective lens. This opto-ACh stimulus was delivered in a frequency-accommodating (50-10 Hz) eight pulse train to stimulate cholinergic axons [52,53] to mimic the activation pattern of cholinergic neurons [54–56]. This opto-ACh protocol elicits direct cholinergic inward current responses resilient to

combined application of glutamatergic synaptic blockers [52,53,57,58] and sensitive to combined cholinergic receptor antagonists [52].

Experimental design, analysis, and statistics

Animals of both sexes were used in pharmacological interventions. All experiments draw on multiple rodents per interventions, and recordings were made from 1 to 3 neurons per brain slice, (brain slices of prefrontal cortex in mouse: 2-3 slices; rat: 3-4 slices). Pharmacological agents were pre-applied for 10 min and co-applied during optogenetic stimuli or exogenous acetylcholine bath application and recovery period. Atropine (200 nM; Sigma-Aldrich) was applied to block muscarinic receptors; dihydro-β-erythroidine (DHβE; 3 μM) to block β2-containing nicotinic receptors; AF-DX 116 (300 nM) to block M2 muscarinic receptors; galantamine hydrobromide (1 μM) to block acetylcholinesterase, and NS9283 (1 μM) to potentiate nicotinic responses. Compounds from Tocris Biosciences unless otherwise specified.

Data analysis was performed in Clampfit 10.3 (Molecular Devices) and Axograph and statistical analysis was performed with Graphpad Prism 10. To measure fast-onset kinetics, raw traces were used for calculating rising slope of current response within 50 ms of opto-ACh onset. To measure response magnitude, downsampled traces were used to fit triple exponentials to opto-ACh responses, from which the peak amplitude (pA) and decay constant (s), where applicable, were measured.

Firing rise is measured by the mean increase in firing frequency for the initial 0.5 s following the onset of the opto-ACh stimulus relative to the mean baseline firing frequency (calculated over 2 s before opto-ACh stimulus). Peak firing frequency is measured as the difference between the mean baseline firing frequency and fastest instantaneous firing frequency following opto-ACh stimulus. Genotype differences between opto-ACh responses were assessed with unpaired two-tailed *t*-tests.

To measure currents to exogenous ACh, 1mM ACh was bath-applied for 15 s. Genotype differences in acetylcholine current magnitude were measured by peak amplitude. Acetylcholine firing response was measured by the time from stimulus onset to peak firing. Both measures are graphed with a cumulative frequency distribution with 10 pA or 10 s bin width, allowing for direct comparison of each age group's genotype differences. Genotype differences in these measures are calculated with a nonparametric Kolmogorov Smirnov (KS) test. Pharmacological manipulations to assess synaptic components of the cholinergic response are calculated with unpaired, two-tailed *t*-tests. The effects of therapeutic interventions are assessed with paired, two-tailed *t*-tests.

Results

Increased opto-ACh responses in early to mid-disease in TgCRND8 AD mouse model

To measure functional changes in cholinergic signals in an AD model, we record whole-cell responses to endogenous acetylcholine released optogenetically (opto-ACh; Fig 1A.1, A.2) in littermate non-transgenic control and TgCRND8 AD mice during early to mid-pathology [42–46]. We find a significant increase in opto-ACh current responses in the AD mice (Fig 1B), as measured by a significantly greater rise slope (Fig 1C, unpaired, two-tailed *t*-test: $t = 3.3$, $P =$

0.002, df = 68) and peak amplitude (Fig 1D, unpaired, two-tailed *t*-test: $t = 3$, $P = 0.004$, df = 68) in AD responses.

This upregulation also can be detected in the change in the firing response elicited by opto-ACh (Fig 1E). Holding the neurons in current clamp and injecting current to elicit ~2-3 Hz action potential firing at baseline, opto-ACh elicits a significantly greater increase in the delta initial firing frequency or firing rise (1F, unpaired, two-tailed *t*-test: $t = 4.2$, $P < 0.0001$, df = 54) and the delta peak firing frequency (1G, unpaired, two-tailed *t*-test: $t = 2.3$, $P = 0.02$, df = 54) in AD compared to control.

These genotype differences are observed in the absence of corresponding genotype differences in passive properties (Supplemental Table 1).

To ask what happens to the AD cholinergic response as neuropathology progresses, we recorded from age- and sex-matched littermate non-transgenic control and TgCRND8 AD mice at a more advanced stage of AD. In this older group, opto-ACh current responses in AD mice are similar to the non-transgenic level (Fig 2A-C; unpaired, two-tailed *t*-test: rise slope $t = 0.07$, $P = 0.9$, df = 75; peak amplitude $t = 0.5$, $P = 0.6$, df = 75) as well as opto-ACh firing responses (Fig 2D-F; unpaired, two-tailed *t*-test: firing rise $t = 0.6$, $P = 0.6$, df = 60; peak firing $t = 0.2$, $P = 0.8$, df = 60). Cholinergic responses in the model are no longer significantly greater than controls at the later time point.

These results suggest that prefrontal endogenous cholinergic responses are upregulated in AD beyond WT levels in early/mid-pathology but that this high level is not maintained above non-transgenic controls when the AD model reaches later disease.

Increased cholinergic responses at mid disease in TgF344 AD rat model

To evaluate whether cholinergic upregulation in response to AD pathology is recapitulated across species, we consider the TgF344-AD rat model [47]. We compared TgF344-AD and littermate WT controls at three points in disease: early AD, mid AD, and later AD [48–51]. Strikingly, we again find an upregulation in cholinergic currents in TgF344-AD rats relative to controls (Fig 3A, 3B). This difference is specific to the mid-AD age group (KS test, $P = 0.005$, D = 0.4) (Fig 3C-E). It was not observed in the early AD group (KS test, $P = 0.7$, D = 0.2), nor in the later AD group (KS test, $P = 0.7$, D = 0.2).

A similar pattern is observed for changes in action potential firing in response to cholinergic stimulation (Fig 3F). The TgF344-AD rat model shows an upregulation in cholinergic firing, as measured by the reduced time taken to attain peak firing rate relative to controls at mid AD (Fig 3G-I, KS test, $P = 0.003$, D = 0.4). However, this difference was not observed at early AD (KS test, $P = 0.8$, D = 0.1) nor at later AD (KS test, $P = 1$, D = 0.1).

The differences in cholinergic responses occur in the absence of corresponding differences in intrinsic properties (Supplemental Table 2).

Together, this work shows the replication of the AD upregulation in cholinergic responses in a different species, a different model, and with a different method of cholinergic stimulation. This conserved property underscores the importance of understanding the receptor mechanisms responsible.

Upregulated responses arise from a selectively- increased nicotinic signal

Since we find that AD cholinergic responses are faster and greater amplitude than non-transgenic controls, we hypothesize that increased nicotinic responses underlie the genotype difference, as these ionotropic receptors impart these characteristics to the endogenous response [52,53,57]. To investigate pre-and post-synaptic elements in the intact prefrontal cholinergic synapse, we use the opto-TgCRND8 AD mouse. To investigate the nicotinic receptor contribution to this upregulated opto-ACh response in AD, we pharmacologically block these receptors using the antagonist DHβE (3uM) (Fig 4A). DHBE changes the cholinergic responses in both genotypes (Fig 4B), significantly decreasing the rise speed (paired, two-tailed t-test: $t = 4.3$, $P = 0.0002$, df = 23) and the peak amplitude (paired, two-tailed t-test: $t = 3.5$, $P = 0.002$, df = 23). However, DHBE exerts a greater effect on the AD group, yielding a significantly greater change in rise slope (Fig 4C, unpaired, two-tailed *t*-test, $t = 2.3$, $P = 0.03$, df = 22) and peak amplitude (Fig 4D, unpaired, two-tailed *t*-test, $t = 2.6$, $P = 0.01$, df = 22). These results suggest that increased opto-ACh responses in this preclinical AD model include a prominent upregulation in nicotinic receptor signalling.

We next evaluate whether muscarinic components of the cholinergic synapse are also altered, since G-protein coupled muscarinic receptors contribute both pre- and post-synaptically to prefrontal cholinergic synapses [52]. We block both pre- and postsynaptic muscarinic receptors with the antagonist atropine (200nM; Fig 4E). Atropine changes the cholinergic responses in both genotypes with blockade of presynaptic autoreceptors increasing opto-ACh responses (Fig 4F), without changing the rise slope (Fig 4G; paired, two-tailed *t*-test: $t = 1.1$, $P = 0.3$, df = 22) but increasing peak amplitude (Fig 4H; paired, two-tailed *t*-test: $t = 7.4$, $P < 0.0001$, df = 22). There was not a significant genotype difference in the effects of atropine, which blocks both pre- and post-synaptic muscarinic receptors. Furthermore, targeted block of presynaptic autoreceptors with AF-DX 116 (Fig 4I) also increases opto-ACh responses in both AD and control (Fig 4J), not changing the rise slope (Fig 4K; paired, two-tailed *t*-test: $t = 1.7$, $P = 0.1$, df = 18) but increasing the peak amplitude (Fig 4L; paired, two-tailed *t*-test: $t = 4.2$, $P = 0.005$, df = 18). These findings suggest that neither pre- nor post-synaptic muscarinic receptors are altered to the same degree as nicotinic receptors in this preclinical AD model.

Treatment strategies: acetylcholinesterase inhibition and nicotinic potentiation amplify cholinergic upregulation

To probe the impact of treatment intervention on this upregulated cholinergic signalling, we measure the effects of current standard of care treatments and a novel treatment strategy on the amplitude and kinetics of the AD neuron and non-transgenic control opto-ACh responses from early to mid and later disease in the TgCRND8 AD mouse.

The pro-cognitive standard-of-care treatment galantamine inhibits acetylcholinesterase (Fig 5A), allowing acetylcholine to remain longer at the synapse. Applying galantamine to opto-ACh AD responses trends towards increasing the rise speed (Fig 5C, paired, two-tailed *t*-test, $t = 2.3$, $P = 0.06$, df = 7) and increases peak amplitude (Fig 5D, paired, two-tailed *t*-test, $t = 4.4$, $P = 0.003$, df = 7). However, its greatest impact is to prolong the decay constant (Fig 5E, paired, two-tailed

t-test, $t = 3.6$, $P = 0.008$, df = 7). Galantamine modestly increases the peak response magnitude; however, it prolongs the overall kinetics of the usually brief cholinergic response.

To explore treatment interventions targeted to the specific nicotinic receptor upregulation seen in this AD model, we test the nicotinic-selective positive allosteric modulator (PAM), NS9283 to enhance endogenous cholinergic signalling (Fig 5F). We find NS9283 greatly boosts opto-ACh AD responses (Fig 5G), significantly increasing the rise speed (Fig 5H; paired, two-tailed *t*-test, $t = 2.7$, $P = 0.02$, df = 14) and the peak amplitude (Fig 5I; paired, two-tailed *t*-test, $t = 3.2$, $P = 0.007$, df = 14). Strikingly, these changes occur without changing the decay constant (Fig 5J; paired, two-tailed *t*-test, $t = 1.3$, $P = 0.2$, df = 14) of the opto-ACh response. This intervention strongly amplifies peak response magnitude while retaining the typical rapid and brief response kinetics.

The current standard of care treatment galantamine modestly increases response amplitude (71% ± 16%) and rise speed (35% ± 16%), but at the cost of greatly slowed decay of the cholinergic response (2032% ± 993%). In comparison, the nicotinic specific NS9283 achieves a significant enhancement in rise speed (210% ± 68%), a much greater increase in amplitude (249% ± 87%) and does not significantly alter response decay (82% ± 33%). NS9283 incites a greater increase in response magnitude and better conserves endogenous response timing and kinetics than the broad cholinergic standard of care treatment. We demonstrate it is possible to use a targeted treatment such as NS9283 to further enhance upregulation of this cognitively-crucial signalling pathway.

Discussion

We demonstrate a functional upregulation in prefrontal cholinergic signalling in two preclinical models of AD. Cholinergic upregulation occurs during early to mid-disease progression, in different species models with differing pathology trajectories. Elevated functional nicotinic signalling plays a dominant role, and the apparent compensation is sensitive to further enhancement via pharmacological manipulation. The AD treatment of AChE-inhibition modestly boosts the cholinergic response but distorts its time course. By contrast, targeted nicotinic positive allosteric modulation exerts a strong and significant potentiation with preserved kinetics. Taken together, our results illustrate an active potential mechanism of cognitive compensation and demonstrate an effective approach to amplify and potentially extend it further into the disease process.

Cognitive reserve and neural compensation in AD

Cognitive reserve, or the brain's ability to sustain neurological decline while maintaining cognitive processes, is well documented clinically in aging [12,13,59,60] and in AD [61,62]. The neurophysiological basis for this reserve is of great interest, with emerging work exploring compensatory plasticity in AD [15] including in the prefrontal cortex [63]. In preclinical models, this has been explored across synapses, where dendritic spine loss has been accompanied by potentially compensatory increases in size of remaining spines [64–67] or *de novo* spinogenesis [68–71]. Investigations into the GABAergic system show remodelling of GABAergic neurons [72] or increases in $GABA_B$ levels [73] to potentially compensate for hyperexcitability in AD [72,74]. In the TgF344 AD rat model used here, parvalbumin interneuron neuroplasticity is observed mid-pathology, with coinciding cognitive resilience in executive function and cognitive flexibility [14].

Interestingly, this emergence of neuroplasticity and cognitive resilience coincides with the same mid-disease timepoint as the cholinergic upregulation found here with the same model.

Prefrontal cholinergic signalling is crucial for many of the cognitive functions maintained by cognitive reserve. Molecularly, it is well known that cholinergic neurons and synapses are sensitive and therefore responsive to AD. The cholinergic system's importance as a pathway for cognitive enhancement, behavioural control, and amenability to change in AD positions it as a potentially significant locus for cognitive reserve. This underscores the need to evaluate cholinergic compensation in AD and whether it can be further harnessed to improve cognitive outcomes. Our work builds on this phenomenon of active compensation, providing novel evidence for the involvement of the cholinergic system in these processes.

Cholinergic signalling and synapses in AD

Previous molecular investigations into cholinergic neurons and synapses in AD communicate a trajectory of cholinergic decline, with decreases in both pre- and post-synaptic markers resulting in eventual heterogenous loss of cholinergic neurons in advanced AD [24,25,75–85]. However, much of this characterization is performed later in disease progression, not capturing functional changes at earlier disease points preceding synapse loss [86,87]. Molecular and functional investigation that has been carried out in early to mid-disease mostly consists of swiftly-progressing genetic models of AD that preclude the use of littermate controls [30–36]. To detect and systematically investigate mechanisms of compensatory plasticity, it is essential to use a well-charted model with appropriately-matched non-transgenic controls.

Functional characterisation is vital for understanding synaptic transmission, as there are many elements regulating signalling that may not be captured otherwise. Changes to receptor localization, internalization, phosphorylation, or alternate forms of regulation may all affect signalling. Nicotinic receptors in particular are tightly regulated by the cell, undergoing desensitization by agonism [88,89] and active trafficking pathways [90,91]. Previous work has shown that they are functionally regulated by other synaptic elements such as lynx family proteins [57,92] or protein kinase C by way of muscarinic receptor agonism [52]. The diversity of elements regulating nicotinic receptor signalling provides many potential avenues for this signalling to be harnessed for compensation. This extends to therapeutic options, where flexibility of the functional nicotinic signal positions it as a powerful locus for further cognitive enhancement.

Here, we find an upregulation in cholinergic signalling that emerges after disease onset, at early to mid-disease in two different preclinical models of AD. Our use of models with littermate non-transgenic controls from early to late disease reveals unprecedented cholinergic upregulation and insight into compensation in AD. Strengths of our electrophysiological and opto-physiological approach include functional insight into cholinergic signalling upregulation, identification of this upregulation as specific to nicotinic receptors. We employ this finding to explore current cholinergic as well as nicotinic specific therapy to further enhance this upregulation and find that specific nicotinic therapy further amplifies cholinergic compensation.

Caveats

An important caveat for our work is our interpretation of cholinergic upregulation as a pro-cognitive compensatory change. Cholinergic signalling has long been appreciated to improve cognition [93,94]. Additionally, upregulation in cholinergic signalling in AD emerges in early to mid-disease but does not continue to increase above non-transgenic levels as AD progresses. This

supports that it is not contributing to disease worsening. We found compensation via nicotinic enhancement, but care must be taken in generalizing this receptor specificity across disease models. This insight was gained using the opto-TgCRND8 AD model mouse, as it engages the complete cholinergic synapse, allowing modulation of pre- and postsynaptic elements mediating cholinergic signalling. In the TgF344 AD rat model, we measure cholinergic responses to exogenous acetylcholine, recording postsynaptic cholinergic responses. Postsynaptic nicotinic receptor signalling mediates prefrontal cholinergic responses in both models used [95–98]. Despite the differences in cholinergic stimulation, nicotinic receptor upregulation is consistent with the similarity in upregulation observed in both models. However, species differences and differences in AD etiology between models may contribute to discrepancies in mechanisms of cholinergic upregulation. Tau pathology, which is seen in the TgF344 AD rat model but not in the TgCRND8 AD mouse, contributes to cholinergic loss [99] and cannot be ruled out from interacting with our identified mechanism. Both models used here employ human APP mutations [40,47], resulting in amyloid-driven AD pathologies. Amyloid beta is known to interact with nicotinic receptors, but the nature of this interaction is unclear [100–105]. In our whole-cell recordings in slice, amyloid beta may not persist in the tissue to the same degree that it exists in the brain [106]. While we did not observe any relationship between time *ex vivo* and extent of nicotinic upregulation, it is possible we are underestimating the contribution of soluble amyloid beta to responses. Nevertheless, our investigation uncovers a nicotinic upregulation that may be a form of active compensation in response to AD.

Translational and clinical impact

Deficits in attention and executive function have consequences for other cognitive domains: if you can't attend, you can't encode [107]. It is therefore important to identify mechanisms through which we can improve attention and extend the maintenance of this cognitive domain as much as possible through AD progression. Nicotinic signalling is essential for attention and executive function and has long been a target for enhancing cognition, including in AD [108,109]. Direct stimulation of nicotinic receptors is pro-cognitive in AD [19], potentially protective against amyloid beta [110,111] but complicated by desensitization [88,89,112]. Nicotinic positive allosteric modulators, such as NS9283 used here, present less risk of desensitization [113], and are pro-cognitive preclinically [114,115]. Our results suggest that nicotinic positive allosteric modulation further enhances nicotinic signalling upregulation in AD, potentially promoting pro-cognitive signalling.

Attention and cue-detection are mediated by cholinergic, and specifically nicotinic stimulation of the prefrontal cortex [116–122] and are timescale dependent [123–125]. Configurations of the fast ionotropic nicotinic receptor that include the α5 subunit lead to faster responses to endogenous acetylcholine [53] and contribute to better attentional performance [126]. Acetylcholinesterase inhibitor, a current and long-used AD treatment, enhances all cholinergic signaling: fast, ionotropic nicotinic signal and slower, longer-lasting metabotropic muscarinic signal shown above (Figure 5) and previously [52,53]. While acetylcholinesterase inhibitor imparts some increase in response amplitude, it profoundly slows response decay. Treatments that maintain the endogenous timing of responses, like the nicotinic positive allosteric modulator that increases the pro-attentional rise kinetics, largely amplifies response magnitude, and does not alter the decay might better enhance time-sensitive cognitive functions.

Understanding neural compensation and neurological changes at different disease stages is important for understanding the implications of clinical interventions. Differing levels of

effectiveness of novel AD treatments may result from timing of intervention and the level of neurological changes already set in motion by AD. Adaptations that are pro-cognitive in the presence of AD may have altered outcomes if pathology is resolved. Therefore, it is important to take neurological changes into account when determining treatment strategies.

Conclusion

Overall, we uncover evidence for cholinergic compensation in two preclinical models of AD. In both models, functional upregulation in prefrontal cholinergic signalling occurs in early to mid-AD. Mechanistic investigation reveals increased nicotinic signalling, which is amenable to further upregulation, both by acetylcholinesterase inhibitor and by nicotinic positive allosteric modulation. Harnessing compensatory nicotinic upregulation may be an important treatment strategy to further enhance and preserve cognition in AD.

Declarations

Funding

This work was funded by research grants from the Canadian Institutes of Health (CIHR): MOP 89825, EKL; PRJ153101, EKL and JM. We also acknowledge the support of a CIHR Banting and Best Canada Graduate Scholarship and an Ontario Graduate Scholarship, SKP.

Contributions

Conceptualization, SKP, JM, EKL; Methodology, SKP, SV, EKL; Data acquisition SKP, SV; Analysis, SKP, SQ; Writing, SKP EKL; Review & editing, SKP, SV, JM, EKL; Funding, SKP, JM, EKL; Supervision, JM, EKL. All authors have critically reviewed and approved of the paper.

Acknowledgements

We thank Janice McNabb and Yao-Fang Tan for expert technical assistance, and Madeleine Ridgeway for optimizing analysis of a related dataset.

Availability of data

The datasets generated during and/or analysed during the current study are not publicly available due to agency over intellectual property but are available from the corresponding author on reasonable request.

Competing interests

The authors have no conflicts or competing interests to declare.

References

1. Stern Y. Cognitive reserve in ageing and Alzheimer's disease. Lancet Neurol. 2012;11:1006–1012.
2. Valenzuela MJ, Sachdev P. Brain reserve and dementia: a systematic review. Psychol Med. 2006;36:441–454.
3. Stern Y, Gurland B, Tatemichi TK, Tang MX, Wilder D, Mayeux R. Influence of education and occupation on the incidence of Alzheimer's disease. JAMA. 1994;271:1004–1010.
4. Scarmeas N, Levy G, Tang M-X, Manly J, Stern Y. Influence of leisure activity on the incidence of Alzheimer's Disease. Neurology. 2001;57:2236–2242.
5. Stern Y, Alexander GE, Prohovnik I, Mayeux R. Inverse relationship between education and parietotemporal perfusion deficit in Alzheimer's disease. Ann Neurol. 1992;32:371–375.
6. Stern Y, Alexander GE, Prohovnik I, Stricks L, Link B, Lennon MC, Mayeux R. Relationship between lifetime occupation and parietal flow: implications for a reserve against Alzheimer's disease pathology. Neurology. 1995;45:55–60.
7. Scarmeas N, Zarahn E, Anderson KE, Habeck CG, Hilton J, Flynn J, Marder KS, Bell KL, Sackeim HA, Van Heertum RL, Moeller JR, Stern Y. Association of Life Activities With Cerebral Blood Flow in Alzheimer Disease. Arch Neurol. 2003;60:359–365.
8. Alexander GE, Furey ML, Grady CL, Pietrini P, Brady DR, Mentis MJ, Schapiro MB. Association of premorbid intellectual function with cerebral metabolism in Alzheimer's disease: implications for the cognitive reserve hypothesis. Am J Psychiatry. 1997;154:165–172.
9. Perneczky R, Drzezga A, Diehl-Schmid J, Schmid G, Wohlschläger A, Kars S, Grimmer T, Wagenpfeil S, Monsch A, Kurz A. Schooling mediates brain reserve in Alzheimer's disease: findings of fluoro-deoxy-glucose-positron emission tomography. J Neurol Neurosurg Psychiatry. 2006;77:1060–1063.
10. Roe CM, Xiong C, Miller JP, Morris JC. Education and Alzheimer disease without dementia: support for the cognitive reserve hypothesis. Neurology. 2007;68:223–228.
11. Groot C, van Loenhoud AC, Barkhof F, van Berckel BNM, Koene T, Teunissen CC, Scheltens P, van der Flier WM, Ossenkoppele R. Differential effects of cognitive reserve and brain reserve on cognition in Alzheimer disease. Neurology. 2018;90:e149–e156.
12. Morcom AM, Johnson W. Neural Reorganization and Compensation in Aging. J Cogn Neurosci. 2015;27:1275–1285.
13. Stern Y. What is cognitive reserve? Theory and research application of the reserve concept. J Int Neuropsychol Soc JINS. 2002;8:448–460.
14. Morrone CD, Lai AY, Bishay J, Hill ME, McLaurin J. Parvalbumin neuroplasticity compensates for somatostatin impairment, maintaining cognitive function in Alzheimer's disease. Transl Neurodegener. 2022;11:26.
15. Bhembre N, Bonthron C, Opazo P. Synaptic Compensatory Plasticity in Alzheimer's Disease. J Neurosci. 2023;43:6833–6840.
16. Dalley JW, Theobald DE, Bouger P, Chudasama Y, Cardinal RN, Robbins TW. Cortical cholinergic function and deficits in visual attentional performance in rats following 192 IgG-saporin-induced lesions of the medial prefrontal cortex. Cereb Cortex N Y N 1991. 2004;14:922–932.
17. Dong H, Csernansky CA, Martin MV, Bertchume A, Vallera D, Csernansky JG. Acetylcholinesterase inhibitors ameliorate behavioral deficits in the Tg2576 mouse model of Alzheimer's disease. Psychopharmacology (Berl). 2005;181:145–152.
18. Nagakura A, Shitaka Y, Yarimizu J, Matsuoka N. Characterization of cognitive deficits in a transgenic mouse model of Alzheimer's disease and effects of donepezil and memantine. Eur J Pharmacol. 2013;703:53–61.

19. Nie H, Wang Z, Zhao W, Lu J, Zhang C, Lok K, Wang Y, Shen H, Xu Z, Yin M. New nicotinic analogue ZY-1 enhances cognitive functions in a transgenic mice model of Alzheimer's disease. Neurosci Lett. 2013;537:29–34.
20. Salloway S, Ferris S, Kluger A, Goldman R, Griesing T, Kumar D, Richardson S, Donepezil 401 Study Group. Efficacy of donepezil in mild cognitive impairment: a randomized placebo-controlled trial. Neurology. 2004;63:651–657.
21. Doody RS, Ferris SH, Salloway S, Sun Y, Goldman R, Watkins WE, Xu Y, Murthy AK. Donepezil treatment of patients with MCI: a 48-week randomized, placebo-controlled trial. Neurology. 2009;72:1555–1561.
22. Geula C, Mesulam M-M. Cholinesterases and the pathology of Alzheimer disease. Alzheimer Dis Assoc Disord. 1995;9:23–28.
23. Tan C-C, Yu J-T, Wang H-F, Tan M-S, Meng X-F, Wang C, Jiang T, Zhu X-C, Tan L. Efficacy and safety of donepezil, galantamine, rivastigmine, and memantine for the treatment of Alzheimer's disease: a systematic review and meta-analysis. J Alzheimers Dis JAD. 2014;41:615–631.
24. Teipel SJ, Dyrba M, Ballarini T, Brosseron F, Bruno D, Buerger K, Cosma N-C, Dechent P, Dobisch L, Düzel E, Ewers M, Fliessbach K, Haynes JD, Janowitz D, Kilimann I, Laske C, Maier F, Metzger CD, Munk MH, Peters O, Pomara N, Preis L, Priller J, Ramírez A, Roy N, Scheffler K, Schneider A, Schott BH, Spottke A, Spruth EJ, Wagner M, Wiltfang J, Jessen F, Heneka MT. Association of Cholinergic Basal Forebrain Volume and Functional Connectivity with Markers of Inflammatory Response in the Alzheimer's Disease Spectrum. J Alzheimers Dis JAD. 2022;85:1267–1282.
25. Aghourian M, Legault-Denis C, Soucy J-P, Rosa-Neto P, Gauthier S, Kostikov A, Gravel P, Bédard M-A. Quantification of brain cholinergic denervation in Alzheimer's disease using PET imaging with [18F]-FEOBV. Mol Psychiatry. 2017;22:1531–1538.
26. Burghaus L, Schütz U, Krempel U, de Vos RA, Jansen Steur EN, Wevers A, Lindstrom J, Schröder H. Quantitative assessment of nicotinic acetylcholine receptor proteins in the cerebral cortex of Alzheimer patients. Brain Res Mol Brain Res. 2000;76:385–388.
27. Xhima K, Markham-Coultes K, Nedev H, Heinen S, Saragovi HU, Hynynen K, Aubert I. Focused ultrasound delivery of a selective TrkA agonist rescues cholinergic function in a mouse model of Alzheimer's disease. Sci Adv. 2020;6:eaax6646.
28. Liu W, Li J, Yang M, Ke X, Dai Y, Lin H, Wang S, Chen L, Tao J. Chemical genetic activation of the cholinergic basal forebrain hippocampal circuit rescues memory loss in Alzheimer's disease. Alzheimers Res Ther. 2022;14:53.
29. McKeever PM, Kim T, Hesketh AR, MacNair L, Miletic D, Favrin G, Oliver SG, Zhang Z, St George-Hyslop P, Robertson J. Cholinergic neuron gene expression differences captured by translational profiling in a mouse model of Alzheimer's disease. Neurobiol Aging. 2017;57:104–119.
30. Choi H-J, Park J-H, Jeong YJ, Hwang J-W, Lee S, Lee H, Seol E, Kim I-W, Cha B-Y, Seo J, Moon M, Hoe H-S. Donepezil ameliorates Aβ pathology but not tau pathology in 5xFAD mice. Mol Brain. 2022;15:63.
31. Na D, Zhang J, Beaulac HJ, Piekna-Przybylska D, Nicklas PR, Kiernan AE, White PM. Increased central auditory gain in 5xFAD Alzheimer's disease mice as an early biomarker candidate for Alzheimer's disease diagnosis. Front Neurosci. 2023;17:1106570.
32. Oddo S, Caccamo A, Shepherd JD, Murphy MP, Golde TE, Kayed R, Metherate R, Mattson MP, Akbari Y, LaFerla FM. Triple-transgenic model of Alzheimer's disease with plaques and tangles: intracellular Abeta and synaptic dysfunction. Neuron. 2003;39:409–421.
33. Oakley H, Cole SL, Logan S, Maus E, Shao P, Craft J, Guillozet-Bongaarts A, Ohno M, Disterhoft J, Van Eldik L, Berry R, Vassar R. Intraneuronal β-Amyloid Aggregates, Neurodegeneration, and Neuron Loss in Transgenic Mice with Five Familial Alzheimer's Disease Mutations: Potential Factors in Amyloid Plaque Formation. J Neurosci. 2006;26:10129–10140.

34. Chen C, Wei J, Ma X, Xia B, Shakir N, Zhang JK, Zhang L, Cui Y, Ferguson D, Qiu S, Bai F. Disrupted Maturation of Prefrontal Layer 5 Neuronal Circuits in an Alzheimer's Mouse Model of Amyloid Deposition. Neurosci Bull. 2022. 24 September 2022. https://doi.org/10.1007/s12264-022-00951-5.
35. Chakroborty S, Kim J, Schneider C, Jacobson C, Molgó J, Stutzmann GE. Early Presynaptic and Postsynaptic Calcium Signaling Abnormalities Mask Underlying Synaptic Depression in Presymptomatic Alzheimer's Disease Mice. J Neurosci. 2012;32:8341–8353.
36. Stutzmann GE, Smith I, Caccamo A, Oddo S, Laferla FM, Parker I. Enhanced ryanodine receptor recruitment contributes to Ca2+ disruptions in young, adult, and aged Alzheimer's disease mice. J Neurosci Off J Soc Neurosci. 2006;26:5180–5189.
37. Falangola MF, Nie X, Ward R, Dhiman S, Voltin J, Nietert PJ, Jensen JH. Diffusion MRI detects basal forebrain cholinergic abnormalities in the 3xTg-AD mouse model of Alzheimer's disease. Magn Reson Imaging. 2021;83:1–13.
38. McNerney MW, Heath A, Narayanan SK, Yesavage J. Repetitive Transcranial Magnetic Stimulation Improves Brain-Derived Neurotrophic Factor and Cholinergic Signaling in the 3xTgAD Mouse Model of Alzheimer's Disease. J Alzheimers Dis;86:499–507.
39. Perez SE, He B, Muhammad N, Oh K-J, Fahnestock M, Ikonomovic MD, Mufson EJ. Cholinotrophic basal forebrain system alterations in 3xTg-AD transgenic mice. Neurobiol Dis. 2011;41:338–352.
40. Chishti MA, Yang D-S, Janus C, Phinney AL, Horne P, Pearson J, Strome R, Zuker N, Loukides J, French J, Turner S, Lozza G, Grilli M, Kunicki S, Morissette C, Paquette J, Gervais F, Bergeron C, Fraser PE, Carlson GA, George-Hyslop PS, Westaway D. Early-onset Amyloid Deposition and Cognitive Deficits in Transgenic Mice Expressing a Double Mutant Form of Amyloid Precursor Protein 695. J Biol Chem. 2001;276:21562–21570.
41. Zhao S, Ting JT, Atallah HE, Qiu L, Tan J, Gloss B, Augustine GJ, Deisseroth K, Luo M, Graybiel AM, Feng G. Cell-type Specific Optogenetic Mice for Dissecting Neural Circuitry Function. Nat Methods. 2011;8:745–752.
42. Romberg C, Horner AE, Bussey TJ, Saksida LM. A touch screen-automated cognitive test battery reveals impaired attention, memory abnormalities, and increased response inhibition in the TgCRND8 mouse model of Alzheimer's disease. Neurobiol Aging. 2013;34:731–744.
43. Walker JM, Fowler SW, Miller DK, Sun AY, Weisman GA, Wood WG, Sun GY, Simonyi A, Schachtman TR. Spatial learning and memory impairment and increased locomotion in a transgenic amyloid precursor protein mouse model of Alzheimer's disease. Behav Brain Res. 2011;222:169–175.
44. Steele JW, Brautigam H, Short JA, Sowa A, Shi M, Yadav A, Weaver CM, Westaway D, Fraser PE, St George-Hyslop PH, Gandy S, Hof PR, Dickstein DL. Early fear memory defects are associated with altered synaptic plasticity and molecular architecture in the TgCRND8 Alzheimer's disease mouse model. J Comp Neurol. 2014;522:2319–2335.
45. Hanna A, Iremonger K, Das P, Dickson D, Golde T, Janus C. Age-related increase in amyloid plaque burden is associated with impairment in conditioned fear memory in CRND8 mouse model of amyloidosis. Alzheimers Res Ther. 2012;4:21.
46. Ambrée O, Touma C, Görtz N, Keyvani K, Paulus W, Palme R, Sachser N. Activity changes and marked stereotypic behavior precede Aβ pathology in TgCRND8 Alzheimer mice. Neurobiol Aging. 2006;27:955–964.
47. Cohen RM, Rezai-Zadeh K, Weitz TM, Rentsendorj A, Gate D, Spivak I, Bholat Y, Vasilevko V, Glabe CG, Breunig JJ, Rakic P, Davtyan H, Agadjanyan MG, Kepe V, Barrio JR, Bannykh S, Szekely CA, Pechnick RN, Town T. A transgenic Alzheimer rat with plaques, tau pathology, behavioral impairment, oligomeric aβ, and frank neuronal loss. J Neurosci Off J Soc Neurosci. 2013;33:6245–6256.

48. Saré RM, Cooke SK, Krych L, Zerfas PM, Cohen RM, Smith CB. Behavioral Phenotype in the TgF344-AD Rat Model of Alzheimer's Disease. Front Neurosci. 2020;14:601.
49. Pentkowski NS, Berkowitz LE, Thompson SM, Drake EN, Olguin CR, Clark BJ. Anxiety-like behavior as an early endophenotype in the TgF344-AD rat model of Alzheimer's disease. Neurobiol Aging. 2018;61:169–176.
50. Joo IL, Lai AY, Bazzigaluppi P, Koletar MM, Dorr A, Brown ME, Thomason LAM, Sled JG, McLaurin J, Stefanovic B. Early neurovascular dysfunction in a transgenic rat model of Alzheimer's disease. Sci Rep. 2017;7.
51. Morrone CD, Bazzigaluppi P, Beckett TL, Hill ME, Koletar MM, Stefanovic B, McLaurin J. Regional differences in Alzheimer's disease pathology confound behavioural rescue after amyloid-β attenuation. Brain. 2020;143:359–373.
52. Power SK, Venkatesan S, Lambe EK. Xanomeline restores endogenous nicotinic acetylcholine receptor signaling in mouse prefrontal cortex. Neuropsychopharmacology. 2023;48:671–682.
53. Venkatesan S, Lambe EK. Chrna5 is Essential for a Rapid and Protected Response to Optogenetic Release of Endogenous Acetylcholine in Prefrontal Cortex. J Neurosci Off J Soc Neurosci. 2020;40:7255–7268.
54. Laszlovszky T, Schlingloff D, Hegedüs P, Freund TF, Gulyás A, Kepecs A, Hangya B. Distinct synchronization, cortical coupling and behavioral function of two basal forebrain cholinergic neuron types. Nat Neurosci. 2020;23:992–1003.
55. Unal CT, Golowasch JP, Zaborszky L. Adult mouse basal forebrain harbors two distinct cholinergic populations defined by their electrophysiology. Front Behav Neurosci. 2012;6:21.
56. Lee MG, Hassani OK, Alonso A, Jones BE. Cholinergic Basal Forebrain Neurons Burst with Theta during Waking and Paradoxical Sleep. J Neurosci. 2005;25:4365–4369.
57. Venkatesan S, Chen T, Liu Y, Turner EE, Tripathy SJ, Lambe EK. Chrna5 and lynx prototoxins identify acetylcholine super-responder subplate neurons. iScience. 2023;26:105992.
58. Sparks DW, Tian MK, Sargin D, Venkatesan S, Intson K, Lambe EK. Opposing Cholinergic and Serotonergic Modulation of Layer 6 in Prefrontal Cortex. Front Neural Circuits. 2017;11:107.
59. Cabeza R, Anderson ND, Locantore JK, McIntosh AR. Aging gracefully: compensatory brain activity in high-performing older adults. NeuroImage. 2002;17:1394–1402.
60. Cabeza R. Hemispheric asymmetry reduction in older adults: the HAROLD model. Psychol Aging. 2002;17:85–100.
61. Morbelli S, Perneczky R, Drzezga A, Frisoni GB, Caroli A, van Berckel BNM, Ossenkoppele R, Guedj E, Didic M, Brugnolo A, Naseri M, Sambuceti G, Pagani M, Nobili F. Metabolic networks underlying cognitive reserve in prodromal Alzheimer disease: a European Alzheimer disease consortium project. J Nucl Med Off Publ Soc Nucl Med. 2013;54:894–902.
62. Menardi A, Pascual-Leone A, Fried PJ, Santarnecchi E. The Role of Cognitive Reserve in Alzheimer's Disease and Aging: A Multi-Modal Imaging Review. J Alzheimers Dis JAD. 2018;66:1341–1362.
63. Mathys H, Peng Z, Boix CA, Victor MB, Leary N, Babu S, Abdelhady G, Jiang X, Ng AP, Ghafari K, Kunisky AK, Mantero J, Galani K, Lohia VN, Fortier GE, Lotfi Y, Ivey J, Brown HP, Patel PR, Chakraborty N, Beaudway JI, Imhoff EJ, Keeler CF, McChesney MM, Patel HH, Patel SP, Thai MT, Bennett DA, Kellis M, Tsai L-H. Single-cell atlas reveals correlates of high cognitive function, dementia, and resilience to Alzheimer's disease pathology. Cell. 2023;186:4365-4385.e27.
64. Alonso-Nanclares L, Merino-Serrais P, Gonzalez S, DeFelipe J. Synaptic changes in the dentate gyrus of APP/PS1 transgenic mice revealed by electron microscopy. J Neuropathol Exp Neurol. 2013;72:386–395.
65. Androuin A, Potier B, Nägerl UV, Cattaert D, Danglot L, Thierry M, Youssef I, Triller A, Duyckaerts C, El Hachimi KH, Dutar P, Delatour B, Marty S. Evidence for altered dendritic spine

compartmentalization in Alzheimer's disease and functional effects in a mouse model. Acta Neuropathol (Berl). 2018;135:839–854.
66. Viana da Silva S, Haberl MG, Zhang P, Bethge P, Lemos C, Gonçalves N, Gorlewicz A, Malezieux M, Gonçalves FQ, Grosjean N, Blanchet C, Frick A, Nägerl UV, Cunha RA, Mulle C. Early synaptic deficits in the APP/PS1 mouse model of Alzheimer's disease involve neuronal adenosine A2A receptors. Nat Commun. 2016;7:11915.
67. Neuman KM, Molina-Campos E, Musial TF, Price AL, Oh K-J, Wolke ML, Buss EW, Scheff SW, Mufson EJ, Nicholson DA. Evidence for Alzheimer's disease-linked synapse loss and compensation in mouse and human hippocampal CA1 pyramidal neurons. Brain Struct Funct. 2015;220:3143–3165.
68. Heiss JK, Barrett J, Yu Z, Haas LT, Kostylev MA, Strittmatter SM. Early Activation of Experience-Independent Dendritic Spine Turnover in a Mouse Model of Alzheimer's Disease. Cereb Cortex N Y N 1991. 2017;27:3660–3674.
69. Tosh JL, Rickman M, Rhymes E, Norona FE, Clayton E, Mucke L, Isaacs AM, Fisher EMC, Wiseman FK. The integration site of the APP transgene in the J20 mouse model of Alzheimer's disease. Wellcome Open Res. 2018;2:84.
70. Stephen T-L, Tamagnini F, Piegsa J, Sung K, Harvey J, Oliver-Evans A, Murray TK, Ahmed Z, Hutton ML, Randall A, O'Neill MJ, Jackson JS. Imbalance in the response of pre- and post-synaptic components to amyloidopathy. Sci Rep. 2019;9:14837.
71. Jackson JS, Witton J, Johnson JD, Ahmed Z, Ward M, Randall AD, Hutton ML, Isaac JT, O'Neill MJ, Ashby MC. Altered Synapse Stability in the Early Stages of Tauopathy. Cell Rep. 2017;18:3063–3068.
72. Palop JJ, Chin J, Roberson ED, Wang J, Thwin MT, Bien-Ly N, Yoo J, Ho KO, Yu G-Q, Kreitzer A, Finkbeiner S, Noebels JL, Mucke L. Aberrant excitatory neuronal activity and compensatory remodeling of inhibitory hippocampal circuits in mouse models of Alzheimer's disease. Neuron. 2007;55:697–711.
73. Iwakiri M, Mizukami K, Ikonomovic MD, Ishikawa M, Hidaka S, Abrahamson EE, DeKosky ST, Asada T. Changes in hippocampal GABABR1 subunit expression in Alzheimer's patients: association with Braak staging. Acta Neuropathol (Berl). 2005;109:467–474.
74. Verret L, Mann EO, Hang GB, Barth AMI, Cobos I, Ho K, Devidze N, Masliah E, Kreitzer AC, Mody I, Mucke L, Palop JJ. Inhibitory interneuron deficit links altered network activity and cognitive dysfunction in Alzheimer model. Cell. 2012;149:708–721.
75. Bowen DM, Smith CB, White P, Davison AN. Neurotransmitter-related enzymes and indices of hypoxia in senile dementia and other abiotrophies. Brain J Neurol. 1976;99:459–496.
76. Davies P, Maloney AJ. Selective loss of central cholinergic neurons in Alzheimer's disease. Lancet Lond Engl. 1976;2:1403.
77. Nordberg A, Alafuzoff I, Winblad B. Nicotinic and muscarinic subtypes in the human brain: changes with aging and dementia. J Neurosci Res. 1992;31:103–111.
78. Schröder H, Giacobini E, Struble RG, Zilles K, Maelicke A. Nicotinic cholinoceptive neurons of the frontal cortex are reduced in Alzheimer's disease. Neurobiol Aging. 1991;12:259–262.
79. Court J, Martin-Ruiz C, Piggott M, Spurden D, Griffiths M, Perry E. Nicotinic receptor abnormalities in Alzheimer's disease. Biol Psychiatry. 2001;49:175–184.
80. Teipel SJ, Cavedo E, Hampel H, Grothe MJ, Alzheimer's Disease Neuroimaging Initiative, Alzheimer Precision Medicine Initiative (APMI). Basal Forebrain Volume, but Not Hippocampal Volume, Is a Predictor of Global Cognitive Decline in Patients With Alzheimer's Disease Treated With Cholinesterase Inhibitors. Front Neurol. 2018;9:642.

81. Sassin I, Schultz C, Thal DR, Rüb U, Arai K, Braak E, Braak H. Evolution of Alzheimer's disease-related cytoskeletal changes in the basal nucleus of Meynert. Acta Neuropathol (Berl). 2000;100:259–269.
82. Araujo DM, Lapchak PA, Robitaille Y, Gauthier S, Quirion R. Differential Alteration of Various Cholinergic Markers in Cortical and Subcortical Regions of Human Brain in Alzheimer's Disease. J Neurochem. 1988;50:1914–1923.
83. Cowburn RF, Wiehager B, Ravid R, Winblad B. Acetylcholine muscarinic M2 receptor stimulated [35S]GTP gamma S binding shows regional selective changes in Alzheimer's disease postmortem brain. Neurodegener J Neurodegener Disord Neuroprotection Neuroregeneration. 1996;5:19–26.
84. Nizari S, Carare RO, Romero IA, Hawkes CA. 3D Reconstruction of the Neurovascular Unit Reveals Differential Loss of Cholinergic Innervation in the Cortex and Hippocampus of the Adult Mouse Brain. Front Aging Neurosci. 2019;11:172.
85. Nizari S, Wells JA, Carare RO, Romero IA, Hawkes CA. Loss of cholinergic innervation differentially affects eNOS-mediated blood flow, drainage of Aβ and cerebral amyloid angiopathy in the cortex and hippocampus of adult mice. Acta Neuropathol Commun. 2021;9:12.
86. Tiraboschi P, Hansen LA, Alford M, Masliah E, Thal LJ, Corey-Bloom J. The decline in synapses and cholinergic activity is asynchronous in Alzheimer's disease. Neurology. 2000;55:1278–1283.
87. Davis KL, Mohs RC, Marin D, Purohit DP, Perl DP, Lantz M, Austin G, Haroutunian V. Cholinergic markers in elderly patients with early signs of Alzheimer disease. JAMA. 1999;281:1401–1406.
88. Wang H, Sun X. Desensitized nicotinic receptors in brain. Brain Res Brain Res Rev. 2005;48:420–437.
89. Picciotto MR, Addy NA, Mineur YS, Brunzell DH. It's not "either/or": activation and desensitization of nicotinic acetylcholine receptors both contribute to behaviors related to nicotine addiction and mood. Prog Neurobiol. 2008;84:329–342.
90. Acharya S, Kundu D, Kim K-M. β-Arrestin1 and GPCR kinase2 play permissive roles in Src-mediated endocytosis of α4β2 nicotinic ACh receptors. Br J Pharmacol. 2021;178:3498–3516.
91. Drenan RM, Nashmi R, Imoukhuede P, Just H, McKinney S, Lester HA. Subcellular trafficking, pentameric assembly, and subunit stoichiometry of neuronal nicotinic acetylcholine receptors containing fluorescently labeled alpha6 and beta3 subunits. Mol Pharmacol. 2008;73:27–41.
92. Tekinay AB, Nong Y, Miwa JM, Lieberam I, Ibanez-Tallon I, Greengard P, Heintz N. A role for LYNX2 in anxiety-related behavior. Proc Natl Acad Sci U S A. 2009;106:4477–4482.
93. Klinkenberg I, Sambeth A, Blokland A. Acetylcholine and attention. Behav Brain Res. 2011;221:430–442.
94. Venkatesan S, Jeoung H-S, Chen T, Power SK, Liu Y, Lambe EK. Endogenous Acetylcholine and Its Modulation of Cortical Microcircuits to Enhance Cognition. Curr Top Behav Neurosci. 2020;45:47–69.
95. Dani JA, Bertrand D. Nicotinic Acetylcholine Receptors and Nicotinic Cholinergic Mechanisms of the Central Nervous System. Annu Rev Pharmacol Toxicol. 2007;47:699–729.
96. Parikh V, Ji J, Decker MW, Sarter M. Prefrontal beta2 subunit-containing and alpha7 nicotinic acetylcholine receptors differentially control glutamatergic and cholinergic signaling. J Neurosci Off J Soc Neurosci. 2010;30:3518–3530.
97. Howe WM, Ji J, Parikh V, Williams S, Mocaër E, Trocmé-Thibierge C, Sarter M. Enhancement of attentional performance by selective stimulation of alpha4beta2(*) nAChRs: underlying cholinergic mechanisms. Neuropsychopharmacol Off Publ Am Coll Neuropsychopharmacol. 2010;35:1391–1401.
98. Lambe EK, Olausson P, Horst NK, Taylor JR, Aghajanian GK. Hypocretin and Nicotine Excite the Same Thalamocortical Synapses in Prefrontal Cortex: Correlation with Improved Attention in Rat. J Neurosci. 2005;25:5225–5229.

99. Belarbi K, Burnouf S, Fernandez-Gomez F-J, Desmercières J, Troquier L, Brouillette J, Tsambou L, Grosjean M-E, Caillierez R, Demeyer D, Hamdane M, Schindowski K, Blum D, Buée L. Loss of medial septum cholinergic neurons in THY-Tau22 mouse model: what links with tau pathology? Curr Alzheimer Res. 2011;8:633–638.
100. Dineley KT. Beta-amyloid peptide--nicotinic acetylcholine receptor interaction: the two faces of health and disease. Front Biosci J Virtual Libr. 2007;12:5030–5038.
101. Arora K, Belcaid M, Lantz MJ, Taketa R, Nichols RA. Transcriptome Profile of Nicotinic Receptor-Linked Sensitization of Beta Amyloid Neurotoxicity. Sci Rep. 2020;10:5696.
102. Lamb PW, Melton MA, Yakel JL. Inhibition of neuronal nicotinic acetylcholine receptor channels expressed in Xenopus oocytes by beta-amyloid1-42 peptide. J Mol Neurosci MN. 2005;27:13–21.
103. Pandya A, Yakel JL. Allosteric modulator Desformylflustrabromine relieves the inhibition of α2β2 and α4β2 nicotinic acetylcholine receptors by β-amyloid(1-42) peptide. J Mol Neurosci MN. 2011;45:42–47.
104. Jürgensen S, Ferreira ST. Nicotinic Receptors, Amyloid-β, and Synaptic Failure in Alzheimer's Disease. J Mol Neurosci. 2010;40:221–229.
105. Magdesian MH, Nery AA, Martins AHB, Juliano MA, Juliano L, Ulrich H, Ferreira ST. Peptide blockers of the inhibition of neuronal nicotinic acetylcholine receptors by amyloid beta. J Biol Chem. 2005;280:31085–31090.
106. Waters J. The concentration of soluble extracellular amyloid-β protein in acute brain slices from CRND8 mice. PloS One. 2010;5:e15709.
107. Romberg C, Bussey TJ, Saksida LM. Paying more attention to attention: towards more comprehensive cognitive translation using mouse models of Alzheimer's disease. Brain Res Bull. 2013;92:49–55.
108. Levin ED, McClernon FJ, Rezvani AH. Nicotinic effects on cognitive function: behavioral characterization, pharmacological specification, and anatomic localization. Psychopharmacology (Berl). 2006;184:523–539.
109. Haydar SN, Dunlop J. Neuronal nicotinic acetylcholine receptors - targets for the development of drugs to treat cognitive impairment associated with schizophrenia and Alzheimer's disease. Curr Top Med Chem. 2010;10:144–152.
110. Kihara T, Shimohama S, Sawada H, Kimura J, Kume T, Kochiyama H, Maeda T, Akaike A. Nicotinic receptor stimulation protects neurons against β-amyloid toxicity. Ann Neurol. 1997;42:159–163.
111. Stevens TR, Krueger SR, Fitzsimonds RM, Picciotto MR. Neuroprotection by nicotine in mouse primary cortical cultures involves activation of calcineurin and L-type calcium channel inactivation. J Neurosci Off J Soc Neurosci. 2003;23:10093–10099.
112. Henderson BJ, Lester HA. Inside-out neuropharmacology of nicotinic drugs. Neuropharmacology. 2015;96:178–193.
113. Williams DK, Wang J, Papke RL. Positive allosteric modulators as an approach to nicotinic acetylcholine receptor- targeted therapeutics: advantages and limitations. Biochem Pharmacol. 2011;82:915–930.
114. Grupe M, Grunnet M, Laursen B, Bastlund JF. Neuropharmacological modulation of the P3-like event-related potential in a rat two-tone auditory discrimination task with modafinil and NS9283, a positive allosteric modulator of α4β2 nAChRs. Neuropharmacology. 2014;79:444–455.
115. Timmermann D, Sandager-Nielsen K, Dyhring T, Smith M, Jacobsen A-M, Nielsen E, Grunnet M, Christensen J, Peters D, Kohlhaas K, Olsen G, Ahring P. Augmentation of cognitive function by NS9283, a stoichiometry-dependent positive allosteric modulator of α2- and α4-containing nicotinic acetylcholine receptors. Br J Pharmacol. 2012;167:164–182.
116. Himmelheber AM, Sarter M, Bruno JP. Increases in cortical acetylcholine release during sustained attention performance in rats. Brain Res Cogn Brain Res. 2000;9:313–325.

117. Parikh V, Kozak R, Martinez V, Sarter M. Prefrontal acetylcholine release controls cue detection on multiple time scales. Neuron. 2007;56:141–154.
118. Gritton HJ, Howe WM, Mallory CS, Hetrick VL, Berke JD, Sarter M. Cortical cholinergic signaling controls the detection of cues. Proc Natl Acad Sci. 2016;113:E1089–E1097.
119. Howe WM, Gritton HJ, Lusk NA, Roberts EA, Hetrick VL, Berke JD, Sarter M. Acetylcholine Release in Prefrontal Cortex Promotes Gamma Oscillations and Theta–Gamma Coupling during Cue Detection. J Neurosci. 2017;37:3215–3230.
120. Hahn B, Shoaib M, Stolerman IP. Involvement of the prefrontal cortex but not the dorsal hippocampus in the attention-enhancing effects of nicotine in rats. Psychopharmacology (Berl). 2003;168:271–279.
121. Hahn B, Shoaib M, Stolerman IP. Nicotine-induced enhancement of attention in the five-choice serial reaction time task: the influence of task demands. Psychopharmacology (Berl). 2002;162:129–137.
122. Hahn B. Cross-species evidence that nicotine widens the attentional window. Psychopharmacology (Berl). 2021;238:3559–3568.
123. Sarter M, Lustig C. Cholinergic double duty: cue detection and attentional control. Curr Opin Psychol. 2019;29:102–107.
124. Paolone G, Lee TM, Sarter M. Time to pay attention: attentional performance time-stamped prefrontal cholinergic activation, diurnality, and performance. J Neurosci Off J Soc Neurosci. 2012;32:12115–12128.
125. Meck WH. Neuropharmacology of timing and time perception. Brain Res Cogn Brain Res. 1996;3:227–242.
126. Bailey CDC, De Biasi M, Fletcher PJ, Lambe EK. The Nicotinic Acetylcholine Receptor α5 Subunit Plays a Key Role in Attention Circuitry and Accuracy. J Neurosci Off J Soc Neurosci. 2010;30:9241–9252.

Figure legends

Figure 1. Endogenous opto-ACh responses are upregulated in early to mid-AD
A.1 Image depicts compound transgenic mouse cross between TgCRND8 AD mouse model and ChAT-ChR2 mouse model expressing channelrhodopsin in cholinergic neurons. Image depicts coronal brain section from these mice, showing the recording electrode positioned over layer 6 of the prefrontal cortex. **A.2** Schematic adapted from Power et al., 2023, represents the cholinergic prefrontal synapse receiving optogenetic stimulus (0.5s pulse train of decreasing frequency). Afferents release endogenous acetylcholine (ACh) which binds to nicotinic and muscarinic receptors, exciting postsynaptic pyramidal neurons. **B** Example opto-ACh responses from non-transgenic (nTg) control (black) and TgCRND8 AD (grey) neurons measured in voltage clamp (Vm = -75 mV). Graphs show significant increase in **C** rise speed ($P < 0.01$) and **D** peak amplitude ($P < 0.01$) of opto-ACh currents in TgCRND8 early AD responses relative to age-matched controls (3-6 months old). **E** Example opto-ACh responses from WT control (black) and TgCRND8 AD (grey) neurons measured in current clamp. Graphs show significant increase in **F** firing rise ($P < 0.0001$) and **G** peak firing frequency ($P < 0.05$) of opto-ACh firing responses in TgCRND8 early/mid AD responses relative to age-matched controls.

Figure 2. Cholinergic signaling not different from non-transgenic in late AD
A Example opto-ACh responses from non-transgenic (nTg) control (black) and TgCRND8 AD (grey) neurons later in disease measured in voltage clamp (Vm = -75 mV). Graphs show no difference in **B** rise speed and **C** peak amplitude of opto-ACh currents in TgCRND8 late AD responses relative to age-matched controls. **D** Example opto-ACh responses from WT control (black) and TgCRND8 AD (grey) neurons later in disease measured in current clamp. Graphs show no difference in **E** firing rise and **F** peak firing frequency of opto-ACh firing responses in TgCRND8 late AD responses relative to age-matched controls.

Figure 3. Early cholinergic upregulation conserved in different species and AD model
A Image depicts TgF344 AD rat model and coronal brain section with the recording electrode positioned over layer 6 of the prefrontal cortex. **B** Example responses to exogenous bath-applied acetylcholine from F344 non-transgenic (nTg) control (black) and TgF344 AD (grey) neurons measured in voltage clamp (Vm = -75 mV). Graphs show cumulative frequency of peak amplitude of acetylcholine current is **C** not different at 8 months, **D** is significantly higher for TgF344 AD responses than controls at 12 months ($P < 0.01$), **E** and is not different at 18 months. Insets show the data in scattergram. **F** Example responses to exogenous bath-applied acetylcholine from F344 WT control (black) and TgF344 AD (grey) neurons measured in current clamp. Graphs show cumulative frequency of time to peak firing of acetylcholine response is **G** not different at 8 months, **H** is significantly faster for TgF344 AD responses than controls at 12 months ($P < 0.01$), **I** and is not different at 18 months. Insets show the data in scattergram.

Figure 4. Early cholinergic upregulation in AD model is specific to nicotinic receptor signalling
A Schematic depicts cholinergic synapse in the presence of nicotinic receptor antagonist DHβE. **B** Paired example opto-ACh responses from non-transgenic (nTg) control (black) and TgCRND8 AD (grey) neurons measured in voltage clamp (Vm = -75mV) before and after DHβE. Graphs show that DHβE causes a greater decline in **C** rise speed ($P < 0.05$) and **D** peak amplitude ($P < 0.05$) of opto-ACh currents in TgCRND8 AD responses relative to controls. **E** Schematic depicts cholinergic synapse in the presence of broad muscarinic receptor antagonist atropine. **F** Paired

example opto-ACh responses from non-transgenic (nTg) control (black) and TgCRND8 AD (grey) neurons measured in voltage clamp before and after atropine. Graphs show that atropine elicits changes in **G** rise speed and **H** peak amplitude that are not different between TgCRND8 AD and control responses. **I** Schematic depicts cholinergic synapse in the presence of muscarinic M2 receptor antagonist AF-DX 116. **J** Paired example opto-ACh responses from non-transgenic (nTg) control (black) and TgCRND8 AD (grey) neurons measured in voltage clamp before and after AF-DX 116. Graphs show that AF-DX 116 elicits changes in **K** rise speed and **L** peak amplitude that are not different between TgCRND8 AD and control responses.

Figure 5. Galantamine and a novel nicotinic treatment strategy further enhances cholinergic upregulation in AD model.

A Schematic depicts cholinergic synapse in the presence of acetylcholinesterase inhibitor galantamine. Galantamine slows the degradation of acetylcholine, prolonging its availability at the synapse. **B** Paired example opto-ACh response from a TgCRND8 AD neuron before (grey) and after galantamine (purple). Graphs show that galantamine elicits **C** no change in rise speed but a significant increase in **D** peak amplitude ($P < 0.01$) and **E** response duration, as measured by the decay constant ($P < 0.01$) in TgCRND8 AD responses. **F** Schematic depicts the activation of postsynaptic nicotinic receptors by acetylcholine and the action of nicotinic PAM NS9283 in increasing nicotinic receptor conductance. **G** Paired example opto-ACh responses from a TgCRND8 AD neuron before (grey) and after NS9283 (blue). Graphs show that NS9283 elicits an increase in **H** rise speed ($P < 0.05$) and **I** peak amplitude ($P < 0.001$) **J** with no change in the response duration.

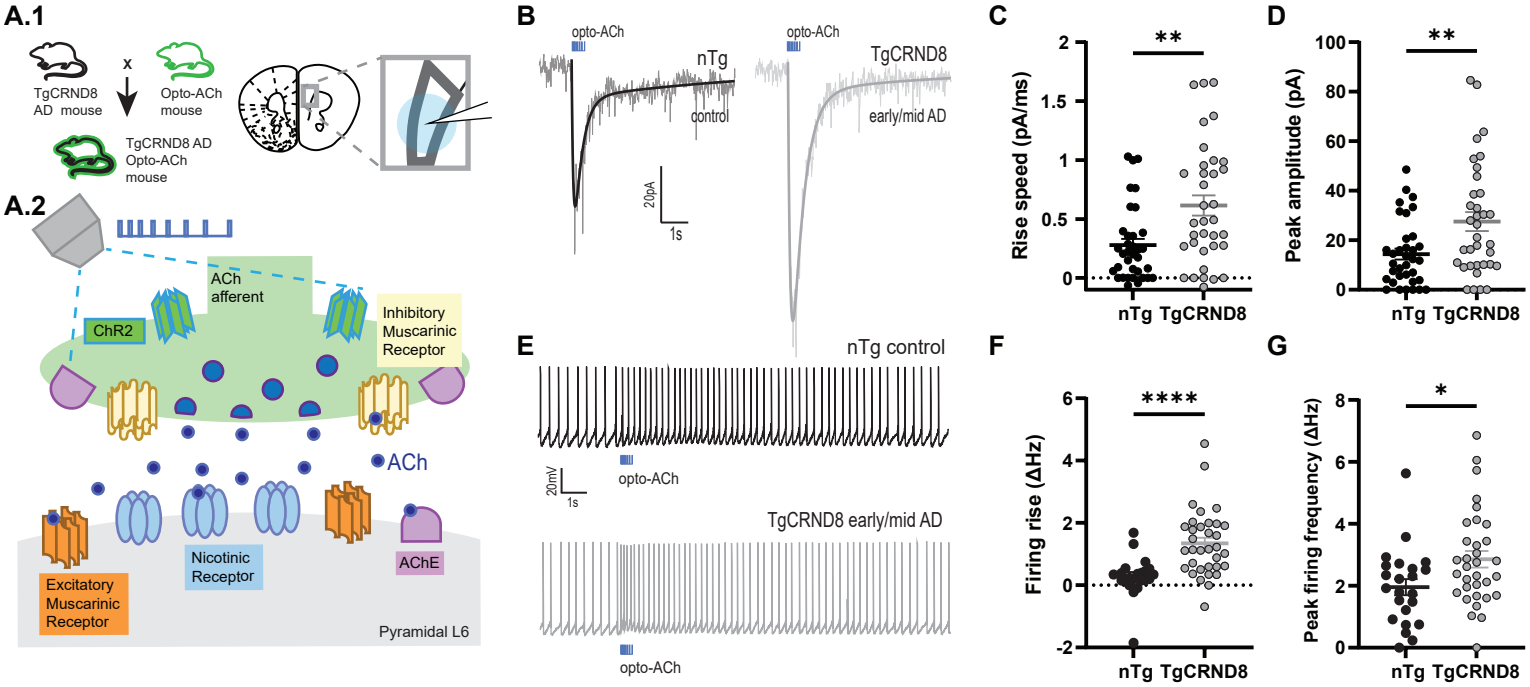

Figure 1. Endogenous opto-ACh responses are upregulated in early to mid-AD

A.1 Image depicts compound transgenic mouse cross between TgCRND8 AD mouse model and ChAT-ChR2 mouse model expressing channelrhodopsin in cholinergic neurons. Image depicts coronal brain section from these mice, showing the recording electrode positioned over layer 6 of the prefrontal cortex. **A.2** Schematic adapted from Power et al., 2023, represents the cholinergic prefrontal synapse receiving optogenetic stimulus (0.5s pulse train of decreasing frequency). Afferents release endogenous acetylcholine (ACh) which binds to nicotinic and muscarinic receptors, exciting postsynaptic pyramidal neurons. **B** Example opto-ACh responses from non-transgenic (nTg) control (black) and TgCRND8 AD (grey) neurons measured in voltage clamp (Vm = -75 mV). Graphs show significant increase in **C** rise speed ($P < 0.01$) and **D** peak amplitude ($P < 0.01$) of opto-ACh currents in TgCRND8 early AD responses relative to age-matched controls (3-6 months old). **E** Example opto-ACh responses from WT control (black) and TgCRND8 AD (grey) neurons measured in current clamp. Graphs show significant increase in **F** firing rise ($P < 0.0001$) and **G** peak firing frequency ($P < 0.05$) of opto-ACh firing responses in TgCRND8 early/mid AD responses relative to age-matched controls.

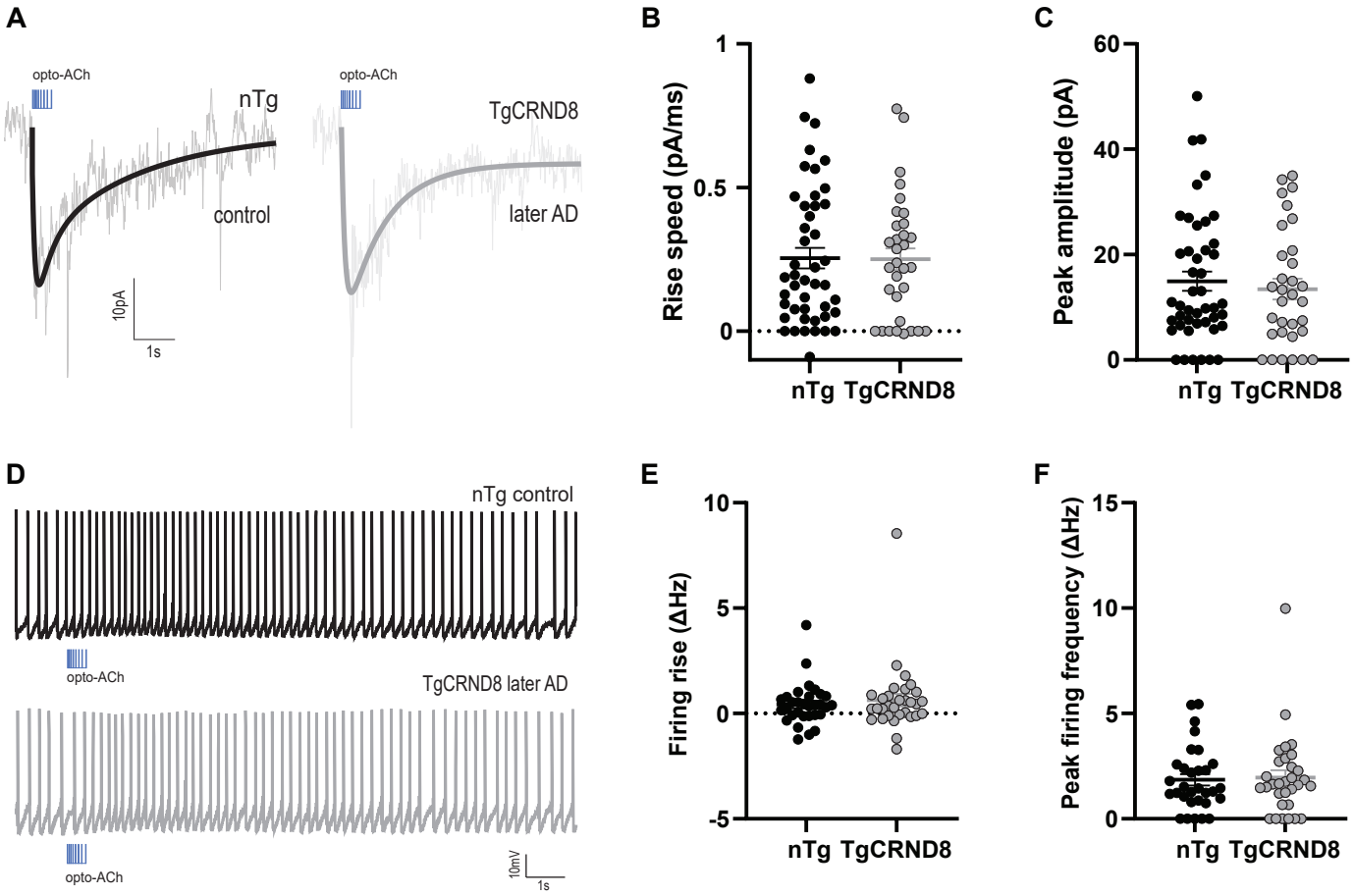

Figure 2. Cholinergic signaling not different from non-transgenic in late AD

A Example opto-ACh responses from non-transgenic (nTg) control (black) and TgCRND8 AD (grey) neurons later in disease measured in voltage clamp (Vm = -75 mV). Graphs show no difference in **B** rise speed and **C** peak amplitude of opto-ACh currents in TgCRND8 late AD responses relative to age-matched controls. **D** Example opto-ACh responses from WT control (black) and TgCRND8 AD (grey) neurons later in disease measured in current clamp. Graphs show no difference in **E** firing rise and **F** peak firing frequency of opto-ACh firing responses in TgCRND8 late AD responses relative to age-matched controls.

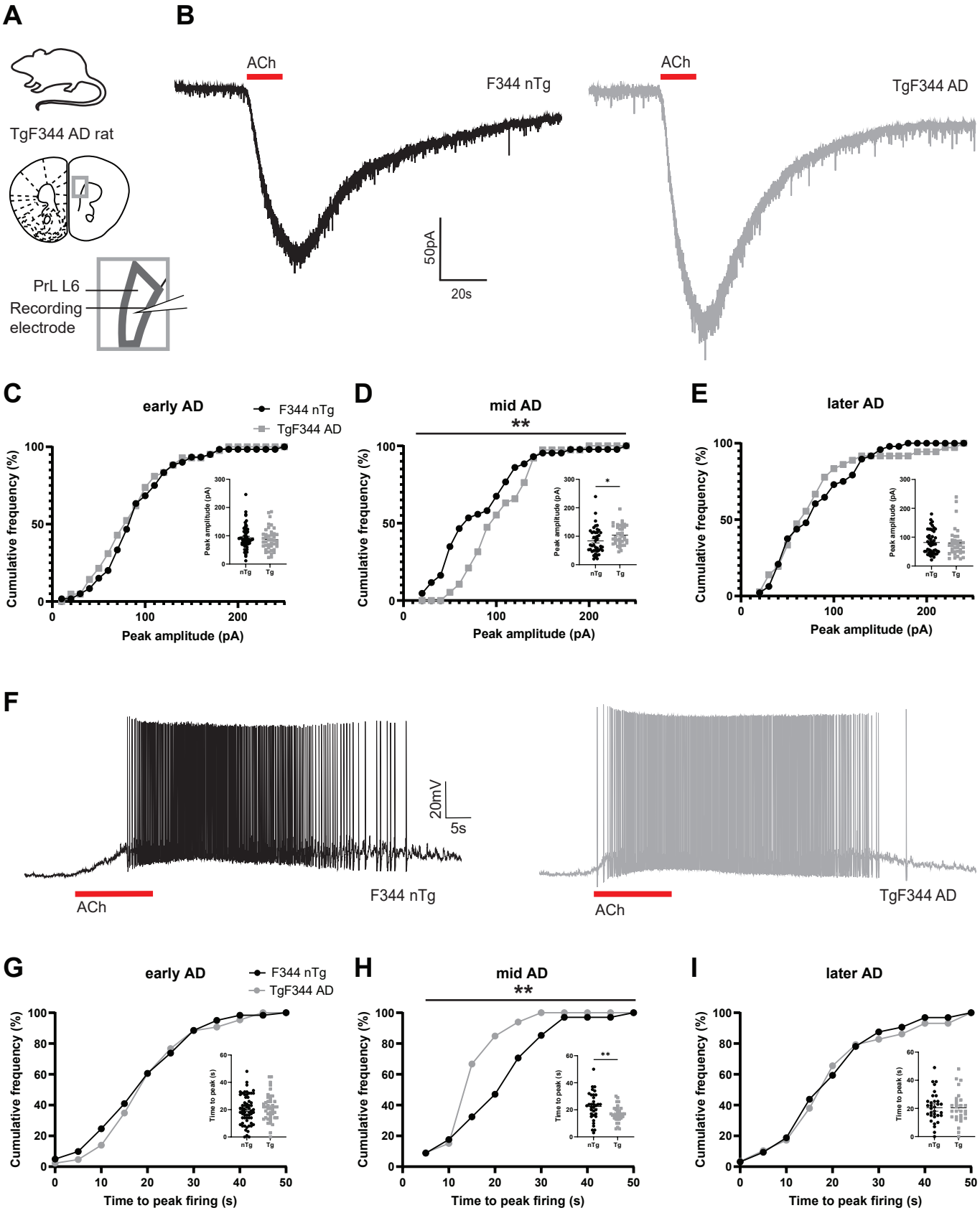

Figure 3. Early cholinergic upregulation conserved in different species and AD model

A Image depicts TgF344 AD rat model and coronal brain section with the recording electrode positioned over layer 6 of the prefrontal cortex. **B** Example responses to exogenous bath-applied acetylcholine from F344 non-transgenic (nTg) control (black) and TgF344 AD (grey) neurons measured in voltage clamp (Vm = -75 mV). Graphs show cumulative frequency of peak amplitude of acetylcholine current is **C** not different at early AD, **D** is significantly higher for TgF344 AD responses than controls at mid AD ($P < 0.01$), **E** and is not different at later AD. Insets show the data in scattergram. **F** Example responses to exogenous bath-applied acetylcholine from F344 WT control (black) and TgF344 AD (grey) neurons measured in current clamp. Graphs show cumulative frequency of time to peak firing of acetylcholine response is **G** not different at early AD, **H** is significantly faster for TgF344 AD responses than controls at mid AD ($P < 0.01$), **I** and is not different at 18 months. Insets show the data in scattergram.

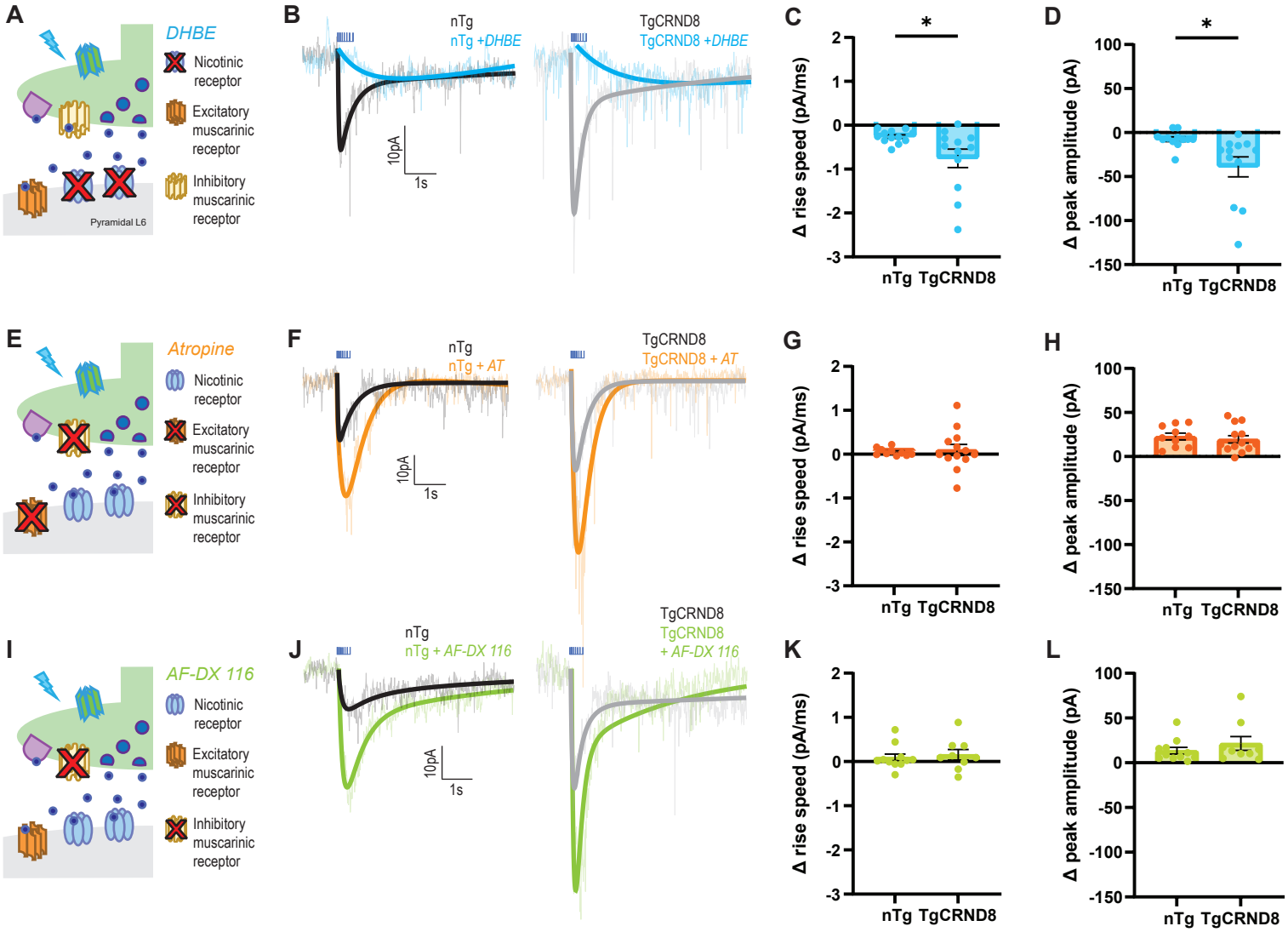

Figure 4. Early cholinergic upregulation in AD is specific to nicotinic receptor signalling

A Schematic depicts cholinergic synapse in the presence of nicotinic receptor antagonist DHβE. **B** Paired example opto-ACh responses from non-transgenic (nTg) control (black) and TgCRND8 AD (grey) neurons measured in voltage clamp (Vm = -75mV) before and after DHβE. Graphs show that DHβE causes a greater decline in **C** rise speed ($P < 0.05$) and **D** peak amplitude ($P < 0.05$) of opto-ACh currents in TgCRND8 AD responses relative to controls. **E** Schematic depicts cholinergic synapse in the presence of broad muscarinic receptor antagonist atropine. **F** Paired example opto-ACh responses from (nTg control (black) and TgCRND8 AD (grey) neurons measured in voltage clamp before and after atropine. Graphs show that atropine elicits changes in **G** rise speed and **H** peak amplitude that are not different between TgCRND8 AD and control responses. **I** Schematic depicts cholinergic synapse in the presence of muscarinic M2 receptor antagonist AF-DX 116. **J** Paired example opto-ACh responses from non-transgenic (nTg) control (black) and TgCRND8 AD (grey) neurons measured in voltage clamp before and after AF-DX 116. Graphs show that AF-DX 116 elicits changes in **K** rise speed and **L** peak amplitude that are not different between TgCRND8 AD and control responses.

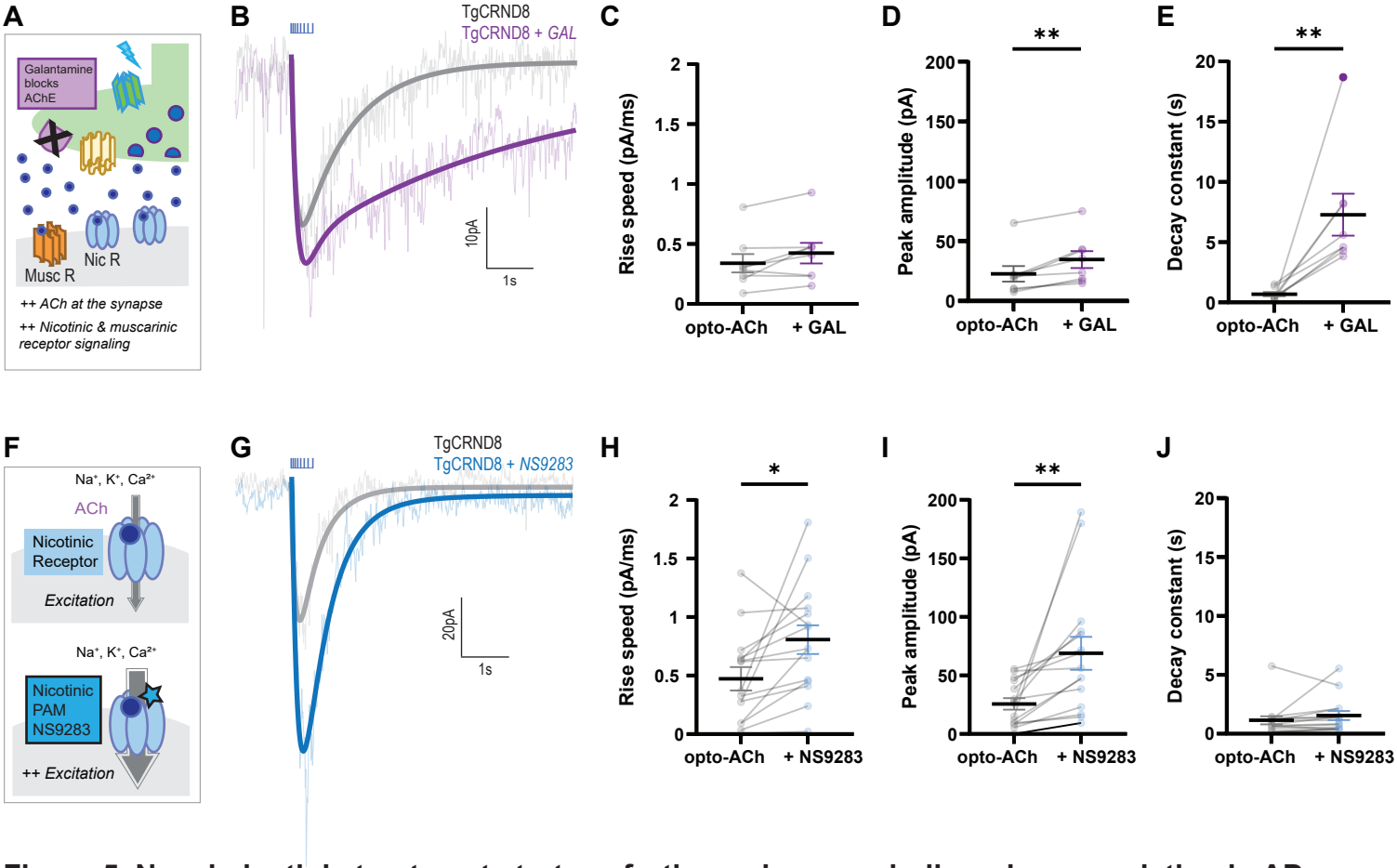

Figure 5. Novel nicotinic treatment strategy further enhances cholinergic upregulation in AD

A Schematic depicts cholinergic synapse in the presence of acetylcholinesterase inhibitor galantamine. Galantamine slows the degradation of acetylcholine, prolonging its availability at the synapse. **B** Paired example opto-ACh response from a TgCRND8 AD neuron before (grey) and after galantamine (purple). Graphs show that galantamine elicits **C** no change in rise speed but a significant increase in **D** peak amplitude ($P < 0.01$) and **E** response duration, as measured by the decay constant ($P < 0.01$) in TgCRND8 AD responses. **F** Schematic depicts the activation of postsynaptic nicotinic receptors by acetylcholine and the action of nicotinic PAM NS9283 in increasing nicotinic receptor conductance. **G** Paired example opto-ACh responses from a TgCRND8 AD neuron before (grey) and after NS9283 (blue). Graphs show that NS9283 elicits an increase in **H** rise speed ($P < 0.05$) and I peak amplitude ($P < 0.001$) **J** with no change in the response duration.